

Composite luminosity function of cluster galaxies

Bianca Garilli¹, Dario Maccagni¹, and Stefano Andreon²

¹ Istituto di Fisica Cosmica G. Occhialini, via Bassini 15, I-20133 Milano, Italy (e-mail: bianca,dario@ifctr.mi.cnr.it)

² Osservatorio Astronomico di Capodimonte, via Moiriello 16, I-80131 Napoli, Italy (e-mail: andreon@na.astro.it)

Received 16 July 1998 / Accepted 12 November 1998

Abstract. We constructed the composite Luminosity Function (LF) of cluster galaxies in the g , r and i bands from the photometry of a mixed (Abell and X-ray selected) sample of the cores of 65 clusters, ranging in redshift from 0.05 to 0.25. The composite LF has been obtained from complete samples of ~ 2200 galaxies in the magnitude range $-23 < M < -17.5$ (-18 in i). Cluster membership has been determined on the basis of color-color plots for each cluster and the resulting outlier counts have been checked against field counts in the same bands. We find that the galaxy density of the environment determines the shape of the LF, in the sense that bright galaxies are more abundant in dense clusters.

Key words: galaxies: clusters: general – galaxies: luminosity function, mass function

1. Introduction

The study of the galaxy luminosity function (LF) in clusters has at least two purposes: (1) to look for differences in the LF of the different clusters, according to their different dynamical status; (2) to compare the galaxy LF in clusters and in the field, and thus to study the influence of the environment on the global statistical properties of the galaxies.

The first cumulative cluster galaxy LF dates back to 1976 (Schechter 1976). Later, Lugger (1983) found that the average LF of 9 clusters was well described by a Schechter function with parameters $M_R^* = -22.74 \pm 0.10$ and $\alpha = -1.27 \pm 0.04$ in the magnitude range $-24.5 < M_R < -20$. Here and in the following we adopt $H_0 = 50 \text{ km s}^{-1} \text{ Mpc}^{-1}$ and $q_0 = 0.5$. All absolute magnitudes have consequently been converted to the long distance scale.

Gaidos (1997) constructed a galaxy LF from R imaging of 20 Abell clusters and also found that it is well described by a Schechter function with parameters $M_R^* = -22.63 \pm 0.11$ and $\alpha = -1.09 \pm 0.08$ in the magnitude range $-24.91 < M_R < -18.91$. Clusters had redshifts in the range $0.06 < z < 0.25$. Gaidos' composite galaxy cluster LF has a slope similar to the field LF derived from the Las Campanas Redshift Survey (Lin et

al. 1996), but the value of M^* is almost one magnitude brighter. To our knowledge this composite cluster galaxy LF is the only one obtained in a red filter from CCD imaging.

Valotto et al. (1997) have computed the cluster galaxy luminosity function in two cluster samples. Galaxy magnitudes have been obtained from the Edinburgh-Durham Southern Galaxy Catalogue (Heydon-Dumbleton, Collins, & MacGillivray 1989), and are thus b_J magnitudes. All clusters lie at $z < 0.07$ and the limiting absolute magnitudes are $M = -17.5$ and $M = -18.5$. For the total sample, the best fitting Schechter function has $M_{b_j}^* = -21.5 \pm 0.1$ and $\alpha = -1.4 \pm 0.1$. There is marginal evidence that in poor clusters galaxies have a flatter LF.

Finally, Lumsden et al. (1997) derive the galaxy LF in the range $-22.5 < M_{b_j} < -19.5$ from a sample of 46 clusters drawn from the Edinburgh/Durham Cluster Catalogue (Lumsden et al. 1992). Cluster redshifts vary from 0.07 to 0.16. The composite LF is derived from 22 of the richer clusters in the sample and has Schechter best fit parameters $M_{b_j}^* = -21.66 \pm 0.02$ and $\alpha = -1.22 \pm 0.04$. Differences in the galaxy LF between different cluster subgroups are found to be weak.

These recent results suggest that galaxy cluster LFs are steeper in the blue than in the red and that their characteristic magnitude is brighter than in the field, by approximately one magnitude in the red (Gaidos 1997 cluster LF with respect to Lin et al. 1996 field LF), and by approximately half a magnitude in the blue (Lumsden et al. 1997 and Valotto et al. 1997 LFs with respect to the ESP field LF (Zucca et al. 1997)).

In this paper, we make use of the multicolor photometric catalog of Abell and *Einstein* Medium Sensitivity Survey (EMSS) clusters of galaxies described in Garilli et al. (1996) to derive the composite galaxy LF in the g , r and i passbands. We must stress that the available cluster imaging is restricted to areas of size close to the cluster cores. The paper is organized as follows: in Sect. 2 we describe the cluster subsample, summarize the photometric technique and discuss the background subtraction; in Sect. 3 we illustrate the method used to construct the composite LFs; in Sect. 4 we present the multicolor LFs obtained for the total sample and for the different cluster subgroups in which the sample can be divided; finally, in Sect. 5 we discuss our results in the light of the recent LF determinations in clusters and in the field.

Send offprint requests to: B. Garilli

Correspondence to: Istituto di Fisica Cosmica G. Occhialini, via Bassini 15, I-20133 Milano, Italy

2. The data

2.1. The cluster sample

The cluster sample used in this work was presented in Tables 1 and 2 of Garilli et al. (1996). In the present work, we excluded 2 clusters (A175 and A410) because their color-color diagrams are anomalous and spectroscopy of a limited number of galaxies in those fields (Bottini et al., in preparation) points to a high background contamination. Three fields, respectively in A1785, A272 and A439, were also excluded from the present analysis because their images are shallower than the average (cf. Table 2 in Garilli et al. 1996).

Finally, galaxies are extracted from 65 clusters, 44 of which are Abell clusters, while the remaining 21 are X-ray selected clusters from the EMSS catalog. The cluster redshift range is $0.05 < z < 0.25$. The average area covered by the CCD images of each cluster has a radius of ~ 350 kpc, but with important variations from cluster to cluster, ranging from ~ 90 to ~ 650 kpc.

2.2. Galaxy photometry

The original photometric catalog from Garilli et al. (1996) was not produced in a fully automatic way. This has some drawbacks when a precise computation of the completeness limit is required. Therefore, we have run SExtractor (Bertin & Arnouts 1996) on the original images, and have compared the results with the original catalogues: the two catalogues are virtually undistinguishable, but for the very faintest objects. Magnitudes in the g , r and i bands have been computed within 10 kpc radii. The choice of a metric aperture magnitude assures the correct computation and comparison of galaxy fluxes and colors in clusters at different redshifts. To allow for comparison with other works (see Sect. 5), isophotal corrected total magnitudes in the r filter have also been computed. Given the spread in z of our cluster sample, k -correction must be applied to get consistent absolute magnitudes. K -corrections depend on spectral type, which, at the zero order, can be assimilated to morphological type. Reliable morphological classifications cannot be derived from our images, but for the brighter galaxies. A possible approach is to assume a morphological composition and apply statistical k -corrections. In our case (small central areas of ~ 350 kpc radius), the morphological composition is highly skewed towards early type galaxies (70% of E+S0 galaxies, Dressler et al. 1997). Moreover, the peak of the redshift distribution is at $z \sim 0.15$, where differences in the k -corrections between ellipticals and spirals are at most 0.1 mag in the g band. Thus, we chose to apply the ellipticals k -corrections (taken from Frei & Gunn 1994) to all galaxies.

2.3. Background subtraction

In the most recent works, background subtraction is performed by counting galaxies in annuli around the cluster positions and statistically subtracting the field contribution to the cluster galaxy counts. Alternatively, when the detector field of view

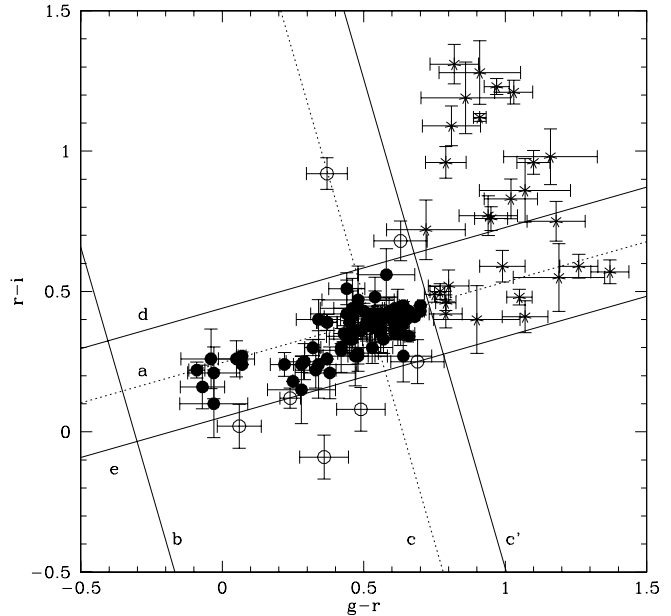


Fig. 1. A typical cluster color-color diagram used to establish cluster membership (see text). Filled dots: cluster member galaxies; starred symbols: background galaxies; open circles: galaxies excluded from membership because too blue or too red in $r - i$ for their $g - r$ color.

is not large enough, flanking fields are obtained from where to infer the local background. Our data do not allow us to follow any of these procedures. However, we have data in three different filters and thus we can exploit colors to remove from each cluster photometric catalog the galaxies with colors not matching the expected ones at the cluster redshift. The method (cf. Garilli, Maccagni & Vettolani 1991, Garilli et al. 1992) assumes that the colors of normal galaxies can be well predicted in this redshift range and therefore galaxies with colors different from the expected ones are interlopers. We followed a procedure which is best illustrated on the basis of Fig. 1. For each cluster, we plot all galaxies brighter than m_{lim} (as defined in Sect. 3.1) in the $g - r$, $r - i$ plane. We define and draw the straight line (line a in Fig. 1) with angular coefficient defined by the k -corrected colors of ellipticals and spirals (Frei & Gunn 1994), offset to match the colors of the three brightest galaxies in the cluster field (assumed to be ellipticals) in order to take into account the possible color shift with respect to the Virgo color-magnitude relation (Garilli et al. 1996). In the same way, we can compute the expected $g - r$ color of ellipticals: line c is the perpendicular to line a passing through this point, and represents the reddest color beyond which we do not expect to find cluster galaxies. To take into account both dispersion on the expected colors of ellipticals and statistical errors in our data, we compute the distance from line c of all galaxies with an $r - i$ color within 3σ of line a and redder than line c . The dispersion of these distances, combined with the expected dispersion in the $g - r$ colors of ellipticals, assumed to be 0.05 mag, summed to the expected colors of ellipticals, defines line c' : all galaxies redder than this value are rejected. As pointed out in 2.2, we do not expect many spirals in our fields, not to

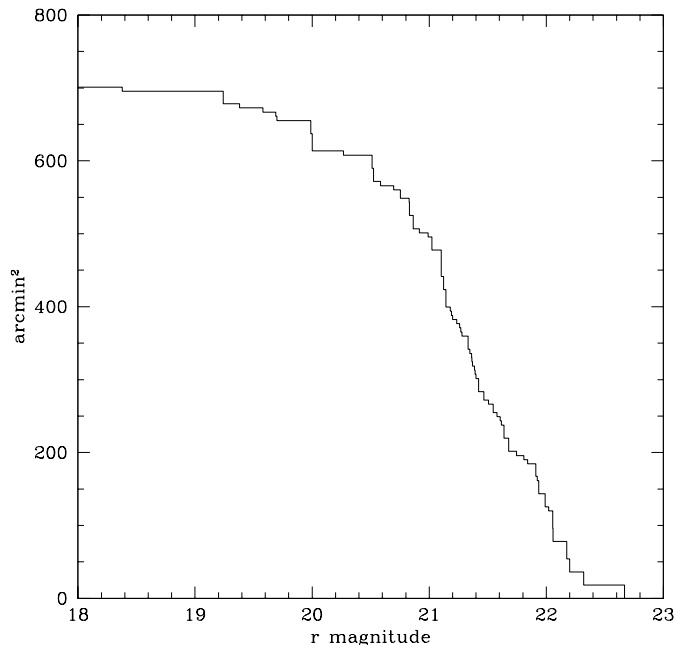


Fig. 2. The area covered by the cluster fields as a function of the r completeness magnitude. The area gently drops for $m_r < 21$, then decreases abruptly.

mention irregulars. On the other hand, we can have some contamination from foreground field galaxies. Depending on their redshift, these galaxies will be found in the bluer part of the diagram. A way to get rid of most of these objects without artificially depleting our clusters of all the spirals they might have, is to compute the minimum expected $\Delta(g-r)$ between spirals and ellipticals at the cluster redshift (Frei & Gunn 1994), and draw line b perpendicularly to line a at that point. All galaxies bluer than line b have a high probability of being interlopers and are therefore rejected. Finally, we compute the robust average distance of galaxies from line a , combine it with the intrinsic color dispersion and determine lines d and e . All galaxies lying outside the horizontal strip defined by lines d and e are rejected.

We then checked the reliability of this method, applied to fields covering the cluster cores, by comparing the results both with spectroscopic measurements and with the field counts obtained in the same photometric system by Neuschaefer & Windhorst (1995). Bottini et al. (in preparation) measured the redshifts of 153 galaxies ($m_r \leq 20$) in several of our sample cluster fields. For 147 galaxies (96%), the assignment based on the color-color technique described above is spectroscopically confirmed (132 cluster members and 15 background galaxies). We erroneously included 4 galaxies (2.5%) and we lost 2 galaxies (1.5%). We can therefore conclude that the adopted color-color background subtraction method gives quite satisfactory results for $m_r \leq 20$. The comparison with the Neuschaefer & Windhorst (1995) field counts is less straightforward because of the varying completeness limits in our fields and consequently of the variation of the surveyed areas as a function of the magnitude. Fig. 2 shows the total surveyed area as a function of the r completeness limit magnitude of the cluster fields. Note that

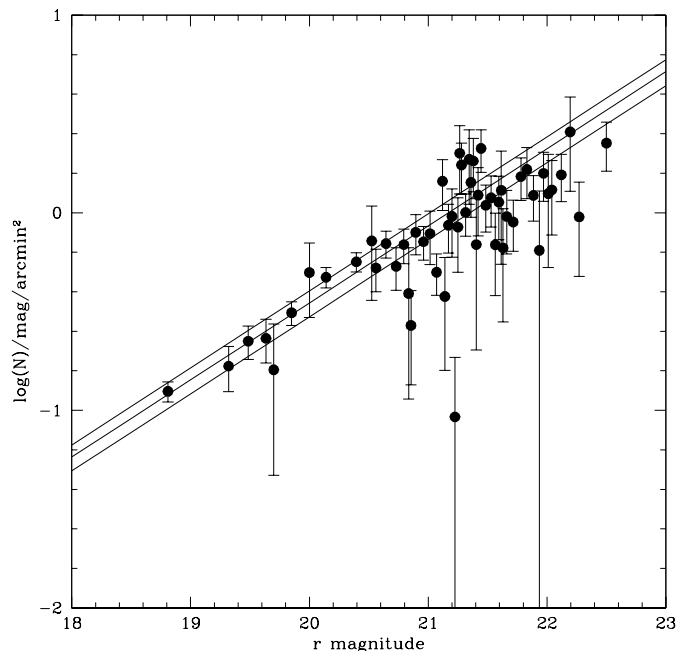


Fig. 3. The r band galaxy counts derived from non member galaxies selected on the basis of the color-color plot of each cluster. Errors are 1σ Poissonian errors over the number of background galaxies in equal area magnitude bins. The continuous straight lines are the field counts obtained by Neuschaefer & Windhorst 1995, where we have considered background fluctuations on the order of 15%.

magnitude bins are not constant. Fig. 3 shows the background counts in magnitude bins of constant area, obtained with the color-color method outlined above, compared with the expected counts in the r band on the basis of the Neuschaefer & Windhorst's (1995) data. According to these authors, field count fluctuations over areas on the order concerning us are $\sim 15\%$, and this is represented in Fig. 3 by the boundary of the strips around the expected value. Errors on our data points (which have not been rebinned) are Poissonian. Inspection of Fig. 3 shows that the background counts we obtain are fully compatible with the field counts of Neuschaefer & Windhorst (1995) up to $m_r = 21$. Up to $m_r = 21.5$, our counts are still compatible, albeit with a larger scatter, while beyond this magnitude the color-color method (applied to these specific fields) probably underestimates the background counts. More quantitatively, in order to perfectly align our background counts to the Neuschaefer & Windhorst's (1995) ones, we should subtract 26 more galaxies (169 have already been considered background) out of a total of 390 in the magnitude bin $21.0 < m_r \leq 21.5$, 54 more galaxies (113 have already been considered background) out of a total of 238 in the magnitude bin $21.5 < m_r \leq 22.0$, and 29 more galaxies (35 have already been considered background) out of a total of 80 in the magnitude bin $22.0 < m_r \leq 22.5$. Note that, in the brighter magnitude bin, the difference is on the same order as the background fluctuations.

Because of the complexity in the construction of the composite luminosity function and of the different limiting magnitude of each cluster catalog, it is difficult to foresee *a priori*

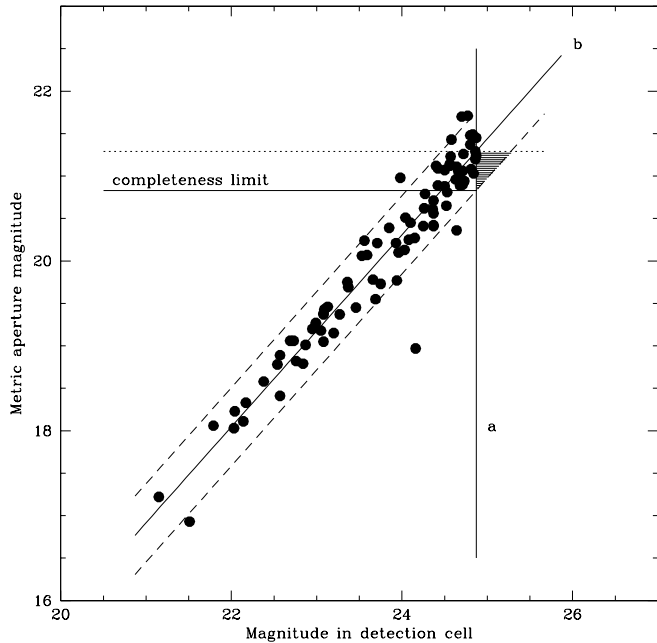


Fig. 4. Determination of the completeness magnitude limit in a fixed aperture given a detection limit (see text) for one of our cluster fields. The completeness limit is given by the intersection of line *a* with the lower envelope of the locus of the detected galaxies.

how the derived luminosity function is affected by an incorrect background subtraction in the faint magnitude range. In order to assess the influence of the uncertainties in the background subtraction on the LF shape, we derived the cluster composite LF from 3 different catalogs. The first one is limited to $m_r = 21$, where both spectroscopy and comparison with field number counts confirm the reliability of our background subtraction procedure. The second one is limited to $m_r = 21.5$, where our field counts still agree within 1σ with the Neuschaefer & Windhorst (1995) counts, and, finally, the third catalog includes all the assumed cluster galaxies.

3. Construction of the composite luminosity function

In order to construct the luminosity function, we need to evaluate two more quantities: the completeness magnitude limit, m_{lim} , and the crowding correction.

3.1. Completeness

Usually, the magnitude completeness is measured through the detectability, as a function of the magnitude, of model galaxies which mimic the two-dimensional surface brightness distribution of real galaxies. In this work, we followed a slightly different approach: we estimated the completeness magnitude limit as the magnitude at which we begin to lose *real galaxies* because they are fainter than our brightness threshold in the detection cell.

The detection limit is set on the magnitude in the detection cell. The correspondence between magnitude in the detection

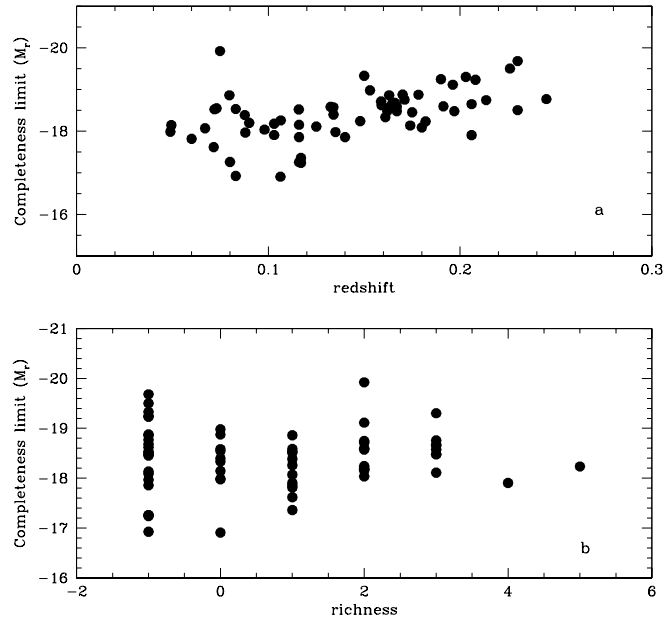


Fig. 5a and b. Aperture absolute magnitude (M_r) completeness limit as a function of redshift **a** and as a function of richness **b** for the whole sample of clusters.

cell and any other magnitude has a certain scatter, which depends essentially on galaxy profile. In Fig. 4, line *a* represents the limit in the detection cell, while line *b* is the linear relation between the magnitude within 10 kpc and the flux within the detection cell (plus and minus 1σ , dashed lines). If the intersection between *a* and *b* (dotted line) were taken as the completeness limit in the metric aperture, it is evident that any galaxy falling in the hatched area would not be detected even if brighter than the completeness limit. These “lost” galaxies become more numerous as the dispersion on line *a* increases, and represent the low surface brightness population. This bias is minimized if, as we did, the dispersion around *b* is taken into account, i.e. if we assume the continuous line as the aperture magnitude completeness limit.

Fig. 5 shows the distribution of absolute magnitudes to which our final cluster galaxy catalogs are complete. There is no trend as a function of cluster richness (b), while a slight trend with redshift is present (a). Fig. 5 (a) shows that only $\sim 10\%$ of the clusters in our sample have completeness limits fainter than $M_r = -17.5$ and that none of the higher redshift clusters has a completeness limit fainter than $M_r = -18$. For the *g* and *i* catalogs, completeness limits for the various clusters have the same behavior. Thus, the LFs we will derive can be considered representative of the cluster sample for magnitudes brighter than $M_r = -17.5$, $M_g = -17.5$, and $M_i = -18$, with the *caveat* that in the fainter bins galaxies are mainly drawn from clusters at $z < 0.15$.

3.2. Crowding correction

An object, to be detected, must satisfy two conditions: its magnitude in the detection cell must be brighter than a given thresh-

old *and* the magnitude contrast with respect to the surroundings must be above a given threshold. This second requirement is necessary to avoid multiple detections in case of resolved structures in the objects, or of noise fluctuations in the halo of large extended objects. When running SExtractor on our fields, this contrast was set at 5.7 mag. Therefore, objects with central surface brightness more than 5.7 mag fainter than the one in which they are embedded are not detected at all. Since our galaxies of lowest central surface brightness are scarcely 5.7 mag fainter than the central surface brightness of bright cluster galaxies, this correction is expected to be negligible for all our measurements, as we verified to be the case.

3.3. The luminosity functions

In most of our clusters there are too few galaxies to determine accurately the shape of the luminosity function. On the contrary, the total number of galaxies in all the cluster sample would allow an accurate evaluation of the composite LF. The most straightforward way to construct a composite LF is to add the single cluster LFs down to the brightest completeness magnitude, or to some other appropriate limit. Obviously, the absolute magnitude range of such an LF will be limited by the shallower of the cluster magnitude limit, which, in our case, would lead to an inefficient use of the available data.

Following Colless' (1989) formulation, we constructed the composite LFs by combining the LFs of all clusters according to:

$$N_{cj} = \frac{1}{m_j} \sum_i N_{ij} w_i$$

where N_{cj} is the number of galaxies in the j th bin of the composite LF, m_j is the number of clusters with limiting magnitude deeper than the j th bin, N_{ij} is the number of galaxies in the j th bin of the i th cluster, and w_i is the weight of each cluster, given by the ratio of the number of galaxies of the i th cluster to the number of galaxies brighter than its magnitude limit in all clusters with fainter magnitude limits.

Our way of constructing the composite LFs differs from Colless' (1989) only in the way the weight of each contributing cluster is computed. In order to make use of all our data base, we weigh clusters on the number of galaxies in an adaptive magnitude range in order to cope with the varying cluster richness and surveyed areas in our sample.

The formal error of the composite LF is computed according to:

$$\sigma_{N_{cj}} = \frac{1}{m_j} \sqrt{\sum_i N_{ij} w_i^2}$$

The final r band complete cluster galaxy catalog respectively contain 2265 galaxies, 2154 of which are brighter than $m_r = 21.5$ and 1971 are brighter than $m_r = 21$. Completeness limits have been evaluated independently in each filter, and since all galaxies brighter than the detection limit in one filter have also been detected in the other filters, our catalogs are complete to the respective magnitude limit independently of the galaxy colors.

Table 1. Full sample: LF best fit Schechter parameters

catalog limiting magnitude	filter	M^*	α	$\chi^2_{red}/d.o.f.$
22.7	r	-21.39 ± 0.10	$-0.87^{+0.10}_{-0.05}$	2.56/10
21.5	r	-21.36 ± 0.10	-0.84 ± 0.08	2.48/10
21.0	r	-21.32 ± 0.10	$-0.82^{+0.10}_{-0.05}$	2.99/9
22.5	g	-21.02 ± 0.10	$-0.87^{+0.04}_{-0.02}$	2.23/10
21.8	g	-20.97 ± 0.10	$-0.82^{+0.05}_{-0.10}$	1.84/10
21.3	g	-20.99 ± 0.10	$-0.83^{+0.08}_{-0.12}$	1.37/10
22.4	i	$-21.67^{+0.05}_{-0.10}$	$-0.87^{+0.10}_{-0.05}$	2.33/10
21.1	i	$-21.62^{+0.05}_{-0.10}$	$-0.83^{+0.08}_{-0.04}$	1.84/10
20.6	i	-21.59 ± 0.10	-0.80 ± 0.10	1.75/10
22.5	r^a	$-22.21^{+0.10}_{-0.15}$	-0.97 ± 0.05	2.16/10
21.5	r^a	$-22.19^{+0.10}_{-0.15}$	$-0.96^{+0.07}_{-0.05}$	2.32/9
21.0	r^a	-22.16 ± 0.15	-0.95 ± 0.07	2.72/9

^a isophotal magnitudes

At the limiting magnitude, the signal to noise ratio is still ~ 15 . The brightest galaxy in each cluster has been removed from the catalogs.

4. Results

We first derived the composite LFs in each filter from each of the apparent magnitude limited galaxy catalogs (see Sect. 2.3). Magnitude limits in the g and i bands have been estimated following the same criteria used for the r band, i.e. compatibility levels with the field counts of Neuschaefer & Windhorst (1995) in the respective filters. The results of the fits with a Schechter function are given in Table 1. For the r filter, we also give the results of the fits when absolute magnitudes are computed from the corrected isophotal magnitudes. As can be seen, the determination of the Schechter parameters is rather robust against the catalogs used. Differences are always within 1σ . In the following, we choose to adopt the Schechter parameterization obtained from the catalogs limited in apparent magnitudes to $m_r = 21.5$, $m_g = 21.8$, and $m_i = 21.1$, which represents a fair compromise between number of galaxies and correctness of background counts estimate.

Fig. 6 (top to bottom) shows the composite luminosity functions in the i , r and g bands (metric aperture magnitudes) obtained from the catalogs limited respectively to 21.1, 21.5 and 21.8 mag, together with the 68 and 90% confidence levels for the M^* , and α parameters resulting from the fit of a Schechter function to the binned data. The normalization is arbitrary. It must be noticed that, although the Schechter function is a fair representation of the composite LF in all three bands, the quality of the fits is rather poor, several points lying more than 1σ from the best fit value.

To search for differences in the LF depending on cluster properties, we have subdivided our data in various ways: galaxies in clusters at $z < 0.15$ and at $z > 0.15$, galaxies in rich

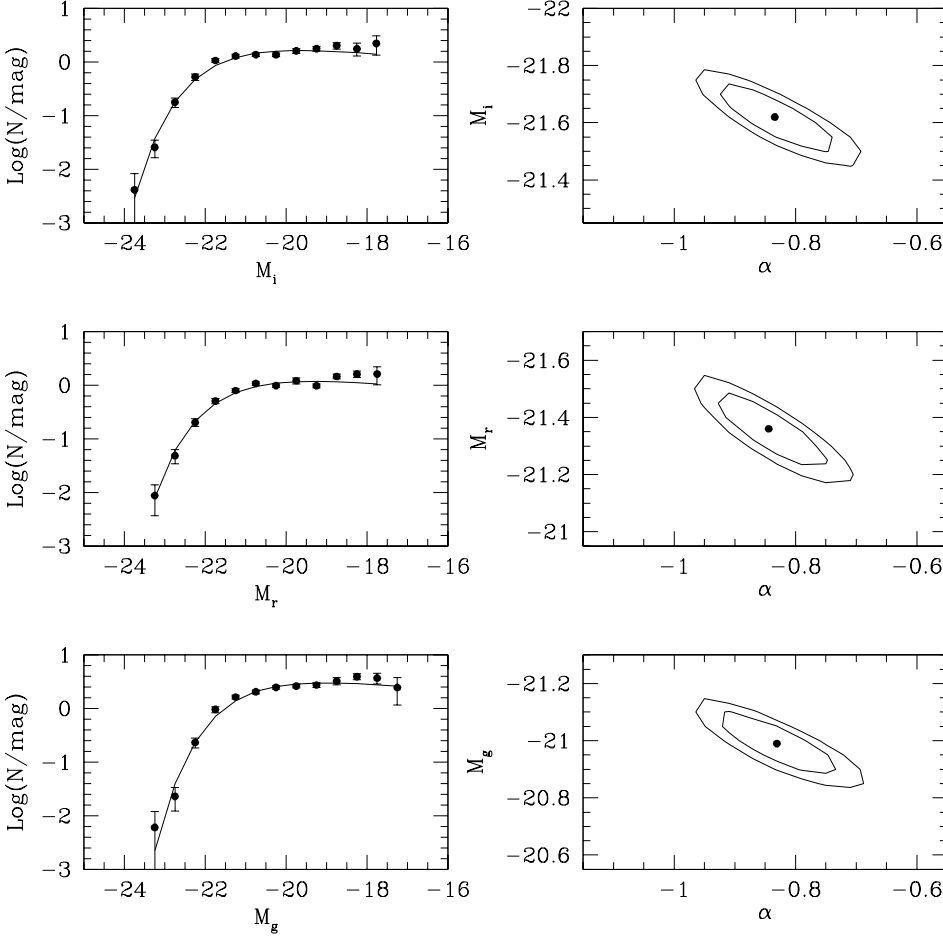


Fig. 6. Composite cluster galaxy LF in the *i*, *r* and *g* bands (left panels) and 90% and 68% confidence contour levels of the best fitting Schechter function parameters. Absolute metric aperture magnitudes have been used. The galaxy catalogs for which the LFs have been derived were limited to $m_i = 21.1$, $m_r = 21.5$, and $m_g = 21.8$.

($R \geq 2$) and poor ($R \leq 1$) clusters (where all EMSS clusters fall in this latter category), galaxies in X-ray selected (EMSS) and in optically selected (Abell) clusters, galaxies in early type (Bautz-Morgan types I and I-II) and later type clusters, and galaxies in *dense* and *loose* clusters. The latter subdivision has been obtained by assuming that all clusters are described by a King (1962) profile

$$S(r) = \frac{S_0}{1 + (r/r_c)^2}$$

where we set $r_c = 250$ kpc. We then computed S_0 by integrating the radially symmetric profile over each cluster field of view and by equating it to number of galaxies brighter than $M_r = -20.1$, roughly corresponding to the magnitude limit utilized by Dressler (1980) to study the morphology–density relation. Clusters have then been divided into *loose* ($S_0 < S_0^{median}$) and *dense* ($S_0 > S_0^{median}$) subsamples, where $S_0^{median} = 74$ galaxies Mpc^{-2} . The average S_0 values of the two groups differ by a factor 2. The composite LFs for the subsamples have been constructed in the same way as for the total sample.

We cannot search for the behavior of the LFs depending on cluster velocity dispersion, as this parameter is missing for most of our clusters.

Table 2 shows the results obtained by fitting a Schechter function to the data subdivided into subsamples.

Table 2. Subsamples: *r* LF best fit Schechter parameters

subsample	M^*	α	M_{limit}	$\frac{\chi_{red}^2}{d.o.f.}$
poor clusters	-21.21 ± 0.10	-0.80 ± 0.10	-18.5	2.28/7
rich clusters	$-21.20^{+0.20}_{-0.10}$	-0.57 ± 0.10	-18.5	1.32/7
<i>loose</i> clusters	-21.50 ± 0.20	$-1.06^{+0.15}_{-0.10}$	-18.0	1.80/8
<i>dense</i> clusters	-21.19 ± 0.10	-0.59 ± 0.10	-18.5	1.63/8
Abell clusters	-21.37 ± 0.10	$-0.81^{+0.05}_{-0.10}$	-18.0	2.83/8
EMSS clusters	-21.11 ± 0.20	-0.82 ± 0.20	-18.0	1.43/8
BM I, I-II	$-21.27^{+0.20}_{-0.10}$	$-0.82^{+0.10}_{-0.15}$	-18.0	2.83/8
BM II, II-III, III	$-21.44^{+0.10}_{-0.20}$	$-0.79^{+0.15}_{-0.05}$	-18.0	1.73/8
$z > 0.15$	-21.20 ± 0.20	$-0.57^{+0.20}_{-0.10}$	-19.0	1.52/6
$z < 0.15$	$-20.98^{+0.20}_{-0.10}$	-0.58 ± 0.15	-19.0	1.75/5

5. Discussion

Let us first consider the LFs of cluster galaxies in the three bands. As can be seen from Fig. 6 (see also Table 1), the *g*, *r* and *i* LFs substantially have the same shape. The magnitude shift of M^* corresponds to the mean color difference of early type galaxies in clusters. The best fitting Schechter function shows a tendency to underestimate the number of galaxies at luminosities around

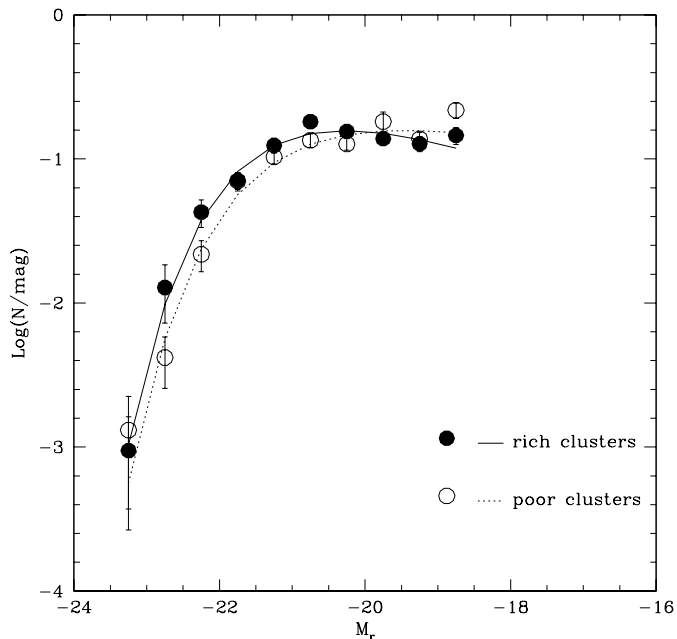


Fig. 7. Composite cluster galaxy LF in the r band for the rich (Abell richness class ≥ 2 (data points: filled dots; best fit Schechter function: continuous line) and poor clusters (data points: open circles; best fit Schechter function: dashed line). Each LF has been normalized to the sum of the number of galaxies in each bin.

$M_r = -21$ and fainter than $M_r = -19$, while it overestimates the number of galaxies with intermediate luminosities. Quite some time ago, Oemler (1974) found slight differences between the LFs of spiral rich and spiral poor clusters. In a sample of 8 clusters, Oegerle & Hoessel (1989) found that the faint end of the LFs varied between < -1 and -1.25 , while the dispersion of M^* was only 0.24 mag. Previously, Lugger (1986) had concluded that the LFs of the 9 clusters she studied formed a rather uniform sample. At the same time, Sandage, Binggeli & Tammann (1985) decomposed the LF of the Virgo galaxies into several morphological components fit by different functions, and recently Biviano et al. (1996) showed that the Coma cluster LF is better fit by a Gaussian and a Schechter function, dominating respectively at the bright and faint end. If the general rule is that different cluster LFs are fit by different Schechter functions or by a combination of Schechter and other functions, it is to be expected that a composite LF would not be nicely fit by a single function. As also Gaidos (1997) noticed in the composite LF he derived, the Schechter function remains a fair representation of the data, but the improved statistics with respect to earlier works shows that the underlying hypothesis of the universality of the cluster LF should probably be abandoned. The cluster morphological mix and the morphology–density relation (Dressler 1980) should give rise to LFs with different shape when subdividing a sample between galaxies in *dense* and *loose* cluster environments, as Lugger (1989) found when constructing the LFs of the inner and outer cluster regions.

Inspection of Table 2 shows that the poor and rich cluster LFs, in this case limited to $M_r = -18.5$, the magnitude of the shallower subsample, differ in α at more than 1σ , while M^*

does not change. The difference, though (see Fig. 7), seems to be due more to a higher ratio of M^* galaxies to fainter ones in rich clusters with respect to poor ones, rather than to a steepening of the poor cluster LF. This same type of difference is enhanced when considering the LFs of cluster galaxies in the *dense* and *loose* subsamples. Fig. 8 shows the LFs of galaxies in loose and dense environments in the three bands. The Schechter fits are quite poor in some cases, especially for the g and r band LFs of the *dense* subsample, and for the r band LF of the *loose* subsample. Galaxies in loose environments show similar LFs (with the expected color shift) in all three bands. In order to quantify the difference in the LFs of *dense* and *loose* cluster galaxies, we can consider the probability of finding a galaxy brighter than -20 mag (-19.5 in the g band). This probability is always $> 30\%$ higher in *dense* clusters. Thus, the density of the environment is a factor which correlates with the galaxy luminosity over a wide range of wavelengths. Not only are cDs found in clusters and nowhere else, but bright galaxies in general are more likely to be found in dense cluster environments. Qualitatively, we can assume that, at some stage of cluster formation, the dense environment stimulates merging or accretion phenomena and the formation of more luminous and, perhaps, more massive galaxies. As already discussed by Lugger (1989), it is not immediate to discriminate among the several phenomena known to occur in clusters (merging, tidal stripping, morphological composition, infall, subclustering), and which could be related to the density parameter. We believe that real progress could be made by investigating galaxy samples in well controlled density environments with photometry extending into the near IR, so that the mass distribution can be studied as well.

We find no evidence of an influence of the dynamical state of clusters on their galaxy LF: early and late B-M types show the same LF, as do Abell and X-ray selected clusters. We are thus led to believe that the cluster evolutionary stage or the selection criterion are factors with little or no impact on the galaxy luminosity, or better, they are not primary factors in determining the luminosity distribution of the constituent galaxies, at least of the giant population in their cores.

The cluster galaxy LFs we obtained in the r band can be directly compared with the one obtained by Gaidos (1997) and the determinations of the LFs measured in the field (apart from a normalization factor). For this and the following comparisons we use the corrected isophotal magnitude instead of the metric aperture magnitude (see Table 1). Furthermore, we assume $m_r = m_{R(KC)} + 0.33$. Our *loose* cluster galaxy LF matches very well Gaidos' LF (the fit with a Schechter function is strikingly similar, see also Fig. 9). Of course, the *dense* cluster galaxy LF differs from Gaidos', since it shows a flatter faint end slope and an excess of bright galaxies. While our results confirm Gaidos' value of M^* in clusters, they also show that this value, or better, the LF shape, is dependent on galaxy density.

In the field, where galaxy density is lower, there are four recent LF determinations in the R band: from the LCRS (Lin et al. 1996), the CNOC1 redshift survey (Lin et al. 1997), the Century Survey (Geller et al. 1997) and the ESO-Sculptor redshift survey (de Lapparent et al. 1997). In Fig. 10 we plot the

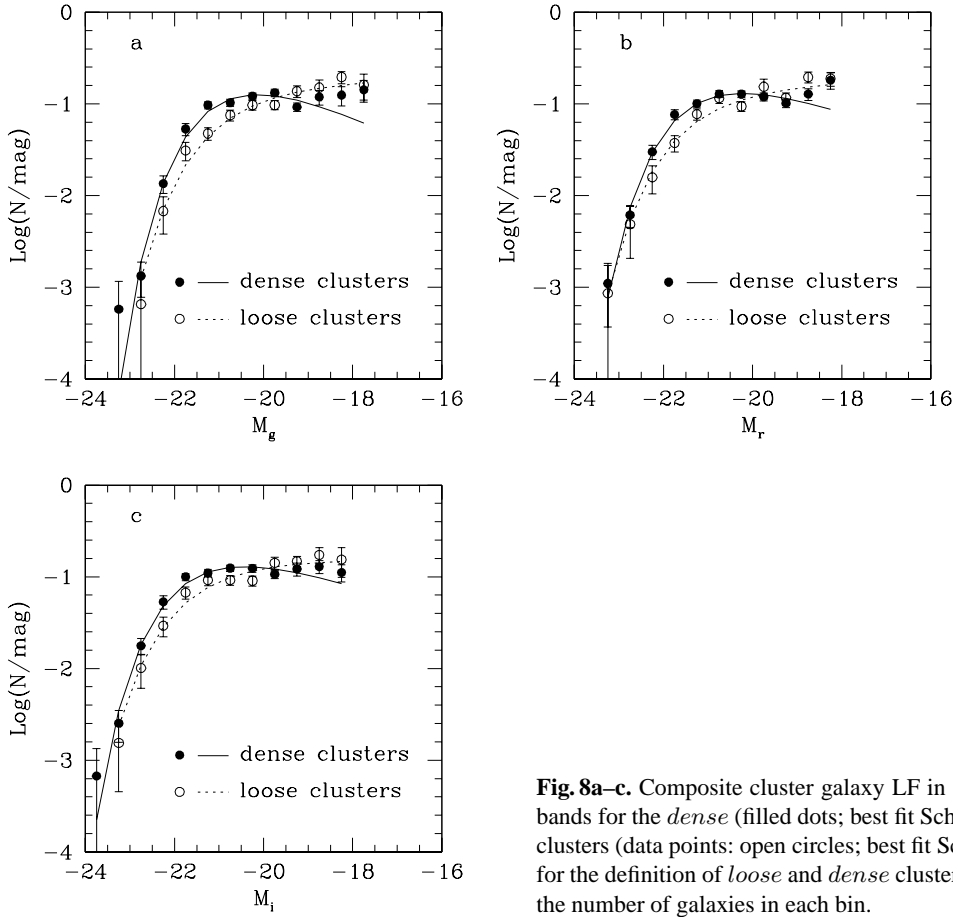


Fig. 8a–c. Composite cluster galaxy LF in the g (panel **a**), r (panel **b**) and i (panel **c**) bands for the *dense* (filled dots; best fit Schechter function: continuous line) and *loose* clusters (data points: open circles; best fit Schechter function: dashed line). See the text for the definition of *loose* and *dense* clusters. Each LF has been normalized to the sum the number of galaxies in each bin.

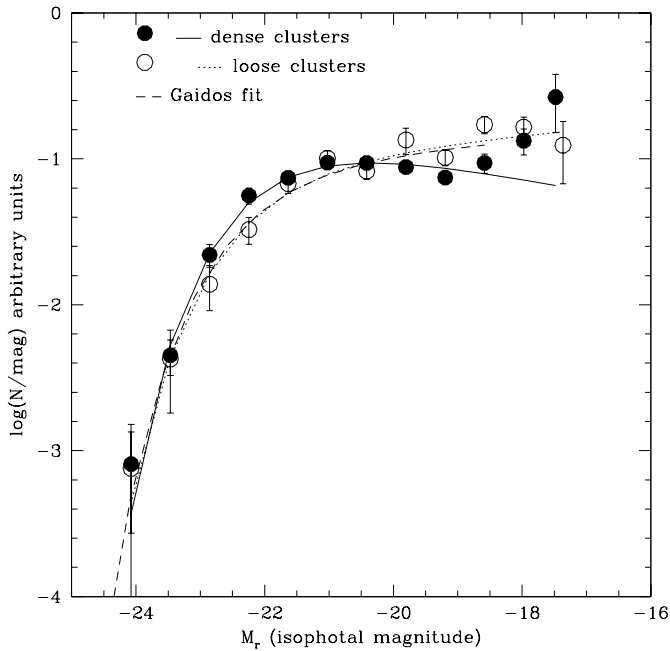


Fig. 9. The composite LF of *loose* and *dense* clusters compared with the one obtained by Gaidos (1997) (long dashed line). Note that in this case we used corrected isophotal magnitudes and not aperture magnitudes.

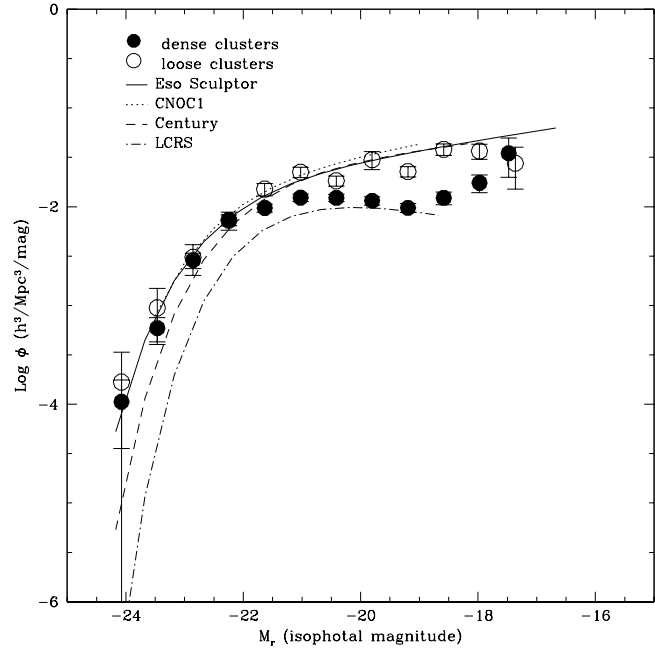


Fig. 10. The composite *loose* and *dense* cluster galaxy LFs we obtained compared with recent determinations of the galaxy LF in the field in the R band. The cluster galaxy LFs have been normalized at M^* (corrected isophotal magnitudes) to the average of the ϕ^* values given for the four field LFs.

four field LFs together with our cluster LFs data points normalized at M^* to the average of the ϕ^* values given for the four field LFs. The *loose* cluster galaxy data points are rather well described by the ESO Sculptor and the CNOC1 LFs, but not so well by the Century LF and even less well by the LCRS LF, which show a lack of bright galaxies. The *dense* cluster galaxy LF is dissimilar from any field galaxy LF, as it is to be expected if the LF is density dependent. We believe that progress on this issue could probably only be obtained by computing the LFs in different density regimes with data showing the same type of selection biases: in this sense the CNOC project seems to be the most promising.

6. Conclusions

We measured a composite cluster galaxy LF in three bands extending over more than 5 magnitudes. We found that the LF of cluster galaxies is dependent on the a measure of the density of the environment. Bright galaxies ($M_r < -20$) have a higher probability of being found in dense clusters. Some recent determinations of the field LF are rather similar to the LF we measure in the less dense clusters.

Acknowledgements. We wish to thank the referee of this paper for the suggestions which prompted us to improve the presentation of the results and of their discussion.

References

- Bertin E., Arnouts S., 1996, A&AS 117, 393
 Biviano A., et al., 1996, A&A 311, 95
 Colless M., 1989, MNRAS 237, 799
 de Lapparent V., Galaz G., Arnouts S., Bardelli S., Ramella M., 1997, The Messenger 89, 21
 Dressler A., 1980, ApJ 236, 351
 Dressler A., et al., 1997, ApJ 490, 577
 Frei Z., Gunn J.E., 1994, AJ 108, 1476
 Gaidos E.J., 1997, AJ 113, 117
 Garilli B., Maccagni D., Vettolani G., 1991, AJ 101, 795
 Garilli B., Bottini D., Maccagni D., Vettolani G., Maccacaro T., 1992, AJ 104, 1290
 Garilli B., Bottini D., Maccagni D., Carrasco L., Recillas E., 1996, ApJS 105, 191
 Geller M.J., et al., 1997, AJ 114, 2205
 Heydon-Dumbleton N.H., Collins C.H., MacGillivray H.T., 1989, MNRAS 238, 379
 King C.R., 1962, AJ 67, 471
 Lugger P., 1986, ApJ 303, 535
 Lugger P., 1989, ApJ 343, 572
 Lin H., Kirshner L.P., Shechtman S.A., et al., 1996, ApJ 464, 60
 Lin H., Yee H.K.C., Carlberg R.G., Ellingson E., 1997, ApJ 475, 494
 Lumsden S.L., Nichol R.C., Collins C.A., Guzzo L., 1992, MNRAS 258, 1
 Lumsden S.L., Collins C.A., Nichol R.C., Eke V.R., Guzzo L., 1997, MNRAS 290, 119
 Neuschaefer L.W., Windhorst R.A., 1995, ApJS 96, 371
 Oegerle W.R., Hoessel J.G., 1989, AJ 98, 1523
 Oemler A. Jr., 1974, ApJ 194, 1
 Schechter P., 1976, ApJ 203, 297
 Sandage A., Binngeli B., Tammann G.A., 1985, AJ 90, 1759
 Valotto C.A., Nicotra M.A., Muriel H., Lambas D.G., 1997, ApJ 479, 90
 Zucca E., et al., 1997, A&A 326, 477